Thermoelastic Investigation of Damage Evolution in Small Stainless Steel Pipework

S. Quinn[1,a], P.J. Tatum[2,b], J.M. Dulieu-Barton[1,c] and R.K. Frühmann[1,d]

[1]School of Engineering Sciences
University of Southampton
Highfield
Southampton
SO17 1BJ
UK

[2]AWE plc
Reading
Berkshire
RG7 4PR
UK

[a]s.quinn@soton.ac.uk, [b]ptatum@awe.co.uk, [c]janice@ship.soton.ac.uk, [d]rkf@soton.ac.uk

ABSTRACT

This paper describes work on damage studies in small cold worked pipe sections. The effect of material heat treatment on the sensitivity of the thermoelastic constant to exposure to plastic strain is assessed. It is shown that strain hardening plays an important role in modifying the thermoelastic constant. X-ray computed tomography has been use to assess the geometry of the deformed cross-section of pipe and to identify the presence of damage. Finally the potential of thermoelastic stress analysis for damage assessment in the pipe work is established.

Introduction

Thermoelastic stress analysis (TSA) is a well-established stress analysis technique [1], based on the measurement of the small temperature change developed in a material as a result of elastic cyclic loading. The temperature change is directly proportional to the change in the sum of the principal surface stresses ($\Delta(\sigma_1 + \sigma_2)$) [2]. This relationship is usually sufficient for linear elastic, homogeneous problems, where the assumption is made that the temperature change is adiabatic.

Recently TSA has been used successfully used to detect and evaluate subsurface damage and flaws [3], by considering information from thermoelastic data over a range of loading frequencies and identifying a non-adiabatic response. In this work damage, in the form of semi-circular notches, was introduced into a flat aluminium plate and thermoelastic data was gathered from the undamaged side of the plate. The local stress gradient in the neighbourhood of the damage was large and lead to non-adiabatic behaviour. This non-adiabatic behaviour was used to reveal the sub surface stresses, by considering the phase information from the thermoelastic signal [3]. In Ref. [3] different damage severities were considered and flaws only a quarter of the thickness of a 5.3 mm thick plate were revealed by the thermoelastic data. The work illustrates the promise of TSA to assess subsurface damage and in the current work this is applied to an industrial problem. The paper describes initial work on the application of TSA in damages studies on small diameter stainless steel pipework.

In earlier work by the authors [4] pipes of cylindrical section, which had an outside diameter of 3.175 mm and an inside diameter of 1.753 mm, i.e. a wall thickness of 0.711 mm, were considered. On assembly the material, 304L quarter hardened stainless steel (UNS S30400), was cold worked by bending around a former. During the product life cycle, maintenance is performed that requires the pipes to be straightened and then bent back to the original shape. To model this operation several specimens, with different deformation histories, of the stainless steel cylindrical section were deformed to shape around a former identical to that used in the assembly process. The bent shape is illustrated in Figure 1, along with the loading arrangement for the TSA tests. The specimens were loaded in bending by applying cyclic compression through the loading blocks shown in Figure 1. (Only one loading block is shown, for clarity, the details are mirrored about the horizontal centreline.) A loading pip was machined in the centre of two flat loading platens and the specimen was loaded in compression through the use of two 5 mm diameter ball bearings.

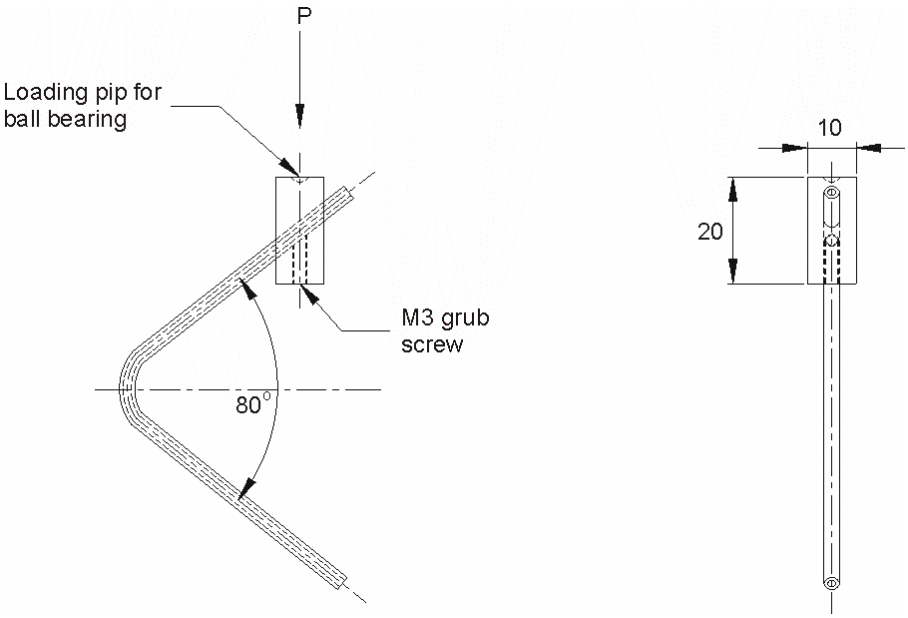

Figure 1. Schematic diagram of the loading arrangement for the deformed pipe tests

In the previous work six pipes with different deformation histories and hence containing different levels of residual stress were tested. It was shown that residual stress does not alter the thermoelastic response of this type of stainless steel. This conclusion was also supported the demonstration that the thermoelastic constant, K, of two specific grades of stainless steel was practically unaltered by plastic strains of up to 20% [4]. This contradicted previous work [5] that showed a monotonic increase in K with increasing levels of plastic strain. However there is a significant difference for the stainless steels considered in Ref. [4], 304L and AISI 321, and the material tested in Ref. [5]: the stainless steels do not strain harden significantly. Therefore it was concluded that strain hardening was the mechanism responsible for the change in the coefficient of linear thermal expansion, α, and hence K. In the first part of the present paper work on an annealed stainless steel is described. This material strain hardens significantly and confirms that exposure to increasing plastic strain with strain hardening has an effect on K.

In Ref. [4] it was identified that failure of the pipe is initiated at the inside of the outer surface of the pipe, by applying a theoretical treatment of how the residual stress profile builds up with increasing numbers of deformation cycles. Any cracking or damage at this inner surface will not be visible so the techniques developed in [3] have been adopted to attempt to reveal information about the damage evolution process at this inner surface for the six specimens with different deformation histories previously considered [4] as well as 3 additional specimens subjected to further deformation cycles. These specimens were inspected at various loading frequencies to investigate the presence of non-adiabatic behaviour that would indicate the presence of any subsurface flaws. One of the imponderables in the previous work [4] was the actual geometry of the deformed shape. Therefore X-ray Computed Tomography (CT) is applied to reveal the actual cross-sectional geometry of the deformed pipe specimens. The CT also provides an indication of the existence of damage at the inner surfaces of the specimens.

Effect of plastic strain on the thermoelastic constant

One of the conclusions from Ref. [4] was that it is necessary for a material to strain harden in order for plastic strain to modify the thermoelastic constant, K. To investigate this further, the procedure described in Ref. [4] is used in the present work to assess the effect of exposure to plastic strain on the thermoelastic response. Therefore it was decided to use similar material to that used in Ref. [4], i.e. AISI 304 stainless steel. However, in this work a solid bar was used instead of cylindrical section, as this facilitates a straight forward measurement of the reduction in cross-sectional area as a result of the permanent set caused by the plastic strain. The material was supplied as rods of 3 mm diameter in the cold drawn condition was annealed in a furnace at a temperature of approximately 1050 ^{o}C for approximately an hour and then air cooled.

An Instron servo-mechanical test machine was used to obtain the stress-strain behaviour of the material in both the as received and annealed conditions. The load was applied in displacement control at a rate of 1 mm/min and the displacement was measured using an electronic extensometer with a gauge length of 50 mm. The outputs from the load cell and the extensometer were recorded during tests to failure to give the stress-strain plots shown in Figure 2. The material properties derived from the plot are as follows for the as received material: yield strength approximately 720 MPa, ultimate tensile strength 804 MPa and elongation to failure of 30.0%. The corresponding values for the annealed material are: yield strength approximately 210 MPa, ultimate tensile strength 597 MPa and elongation to failure 59.6%. The huge difference in the strain hardening characteristics of the two materials is clear from inspection of Figure 2; the as received material strain hardens by approximately 12% and the annealed material strain hardens by 284%.

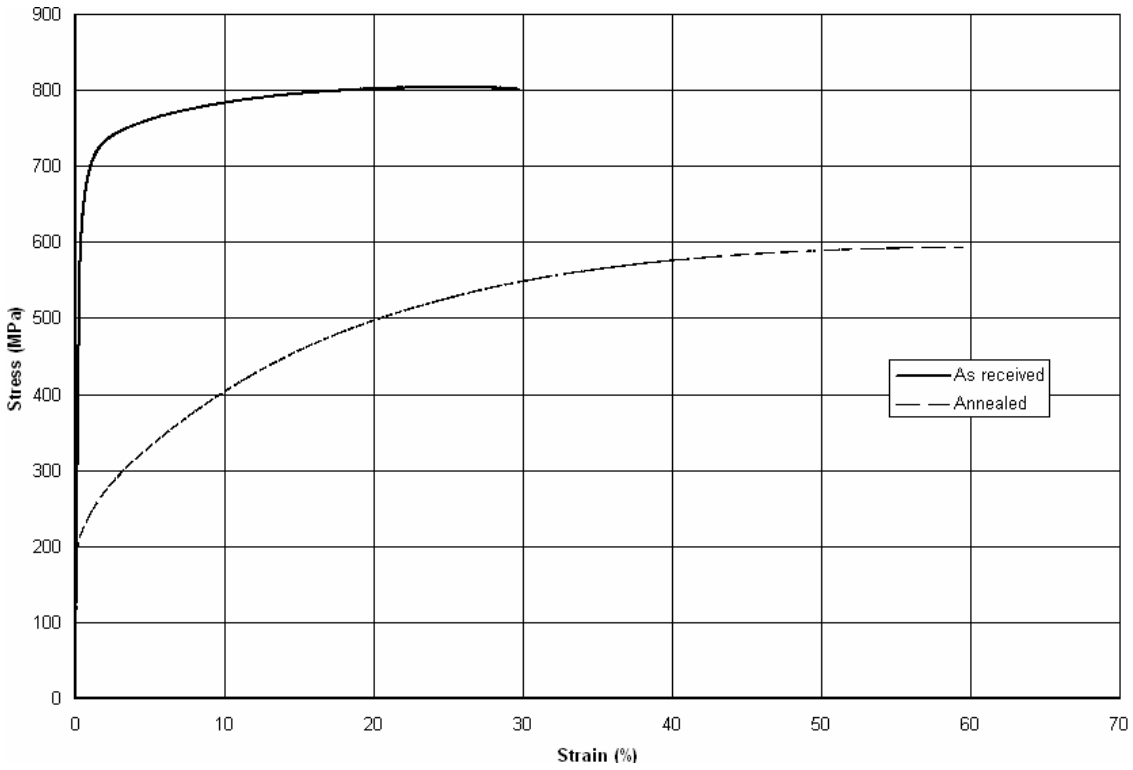

Figure 2. Stress-strain curves for as received and annealed AISI 304 stainless steel

Again, following the test procedures described in full in Ref. [4], the thermoelastic response of the specimen in an unstrained condition was characterised, to determine a baseline thermoelastic signal, S_0. To ensure that the thermoelastic response was linear the applied stress range was increased in 30 MPa increments from 30 to 180 MPa about a mean load of 100 MPa for loading at a constant rate of 5 Hz. By using the zoom lens of the DeltaTherm 1410 system a 15 mm by 15 mm area of data was collected so that an area of approximately 10 by 100 pixels from the 256 by 256 detector array could be used to determine the average signal from the centre of the specimen. The data collection was accumulated over 8 seconds and integrated over a 60 second time period to minimise noise content. Then further specimens were strained statically to maximum strains of approximately 10 and 20% and unloaded for both the as received and annealed material. Thermoelastic images were then collected from the specimens in their strained condition, whilst subjected to a constant applied stress range. The increase in the thermoelastic constant for these levels of plastic strain was then defined, using the following equation [5]

$$\frac{S_s}{S_0} = \frac{K_s}{K_0} \tag{1}$$

Equation (1) is valid when tests are carried out using the same applied stress range, the same detector and the same paint coating. It is also assumed that the specimen surface has the same absolute temperature.

The raw thermoelastic data from these tests is given in Table 1. Although there is a linear relationship between applied stress range and thermoelastic signal at each strain increment the noise in the data at the lower applied stress ranges of 30 and 60 MPa is noticeably larger than for the higher applied stress ranges, see Table 1, and so this data has been neglected from the

plot of K_s/K_0 obtained from equation (1) against residual strain given in Figure 3. The data for the as received material is indicated by the solid diamonds the solid line gives the linear line of best fit through the data. The open squares and the dotted line is the equivalent for the annealed material. Although there is scatter in the results, the general trend is for the thermoelastic constant, K, for the as received material to increase slightly with increasing strain whilst K for the annealed material decreases to a larger extent. The clear reduction in K for the annealed material indicates that the strain hardening does modify the material properties. Therefore it may be concluded that any material that experiences strain hardening can be expected to have a change in K. This provides a possible route for residual stress assessment and current work is focusing on this issue. In the current work this approach cannot be adopted as the material does not significantly strain harden and the change in K shown in Figure 3 is too small to be detected accurately using TSA. Therefore the remainder of this paper will focus on possible departures in the stress field due to geometry changes resulting from the deformation and also the possibility of using a non-adiabatic thermoelastic response to detect damage.

Table 1. Thermoelastic data from the as received and annealed AISI 304 stainless steel material for different maximum applied strains

Applied stress range	As received						Annealed					
	Uncalibrated signal (U)			Coefficient of variation (%)			Uncalibrated signal (U)			Coefficient of variation (%)		
	Maximum strain (%)			Maximum strain (%)			Maximum strain (%)			Maximum strain (%)		
(MPa)	0.0	10.0	20.1	0.0	10.0	20.1	0.0	9.9	20.0	0.0	9.9	20.0
30	1002	949	872	10.5	12.2	9.2	836	917	848	12.6	17.0	11.3
60	2163	2091	1823	5.9	7.3	5.6	1666	1782	1715	6.7	8.8	7.4
90	3248	3479	3256	5.1	6.6	4.9	3052	3002	2796	5.8	4.3	7.0
120	4308	4577	4256	4.9	6.6	4.7	3962	3997	3894	5.6	5.4	6.8
150	5513	5658	5397	4.5	6.5	5.5	5134	5079	4945	5.4	4.0	7.1
180	6564	6590	6556	4.8	7.1	5.3	6013	6055	5945	5.2	3.9	7.4

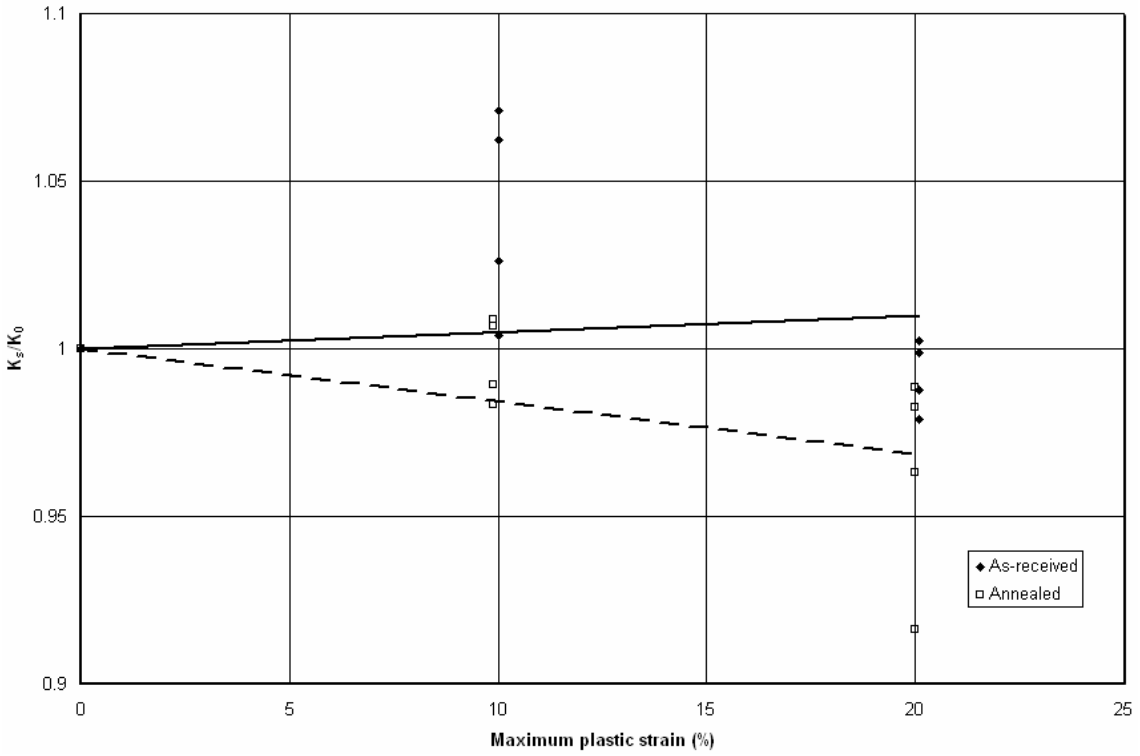

Figure 3. Variation in the thermoelastic constant, K, with maximum plastic strain

X-ray computed tomography of pipe specimens

In the previous work described in Ref. [4] the geometry of the cross-sectional area of the deformed specimens at the bend was estimated from external measurements. Clearly the deformed geometry will affect the stresses and therefore must be

established prior to any quantitative TSA. Therefore the X-ray computed tomography (CT) technique has been used to non-destructively examine the pipe specimens, to show the actual cross-section of the deformed pipe specimens and determine the existence of damage at the inner surfaces of the specimens.

The deformation history details for the pipes considered in the experimental work were as follows: specimen 1 was bent to shape once whilst specimen 3 had been bent to shape, straightened, bent to shape, straightened and bent to shape a third time. Specimens 5, 6, 8, 12 and 16 represented those bent to shape five, six, eight, 12 and 16 times respectively, in a similar manner. In the CT work specimens 1, 6 and 16 were examined. The deformed shape is shown in Figure 1.

An X-tek Systems 'Benchtop CT' machine was used with images were collected at a resolution of approximately 10 μm. X-ray CT images of three pipes, subjected to 1, 6 and 16 deformation cycles, are shown in Figure 4. These X-ray CT images clearly show the gross changes in the cross-section that occur with increasing deformation cycles and the significant flattening of the pipe into an elliptical shape with increasing cold bending cycles. The dimensional data that has been taken from these cross-sectional images is summarised in Table 2. It is also worth noting that even for the specimen that has been subjected to 16 deformation cycles there is no indication of damage at the internal surfaces of the pipe. Based on the resolution of the CT system it can be concluded that there is no damage in the pipes of greater than 10 μm in size.

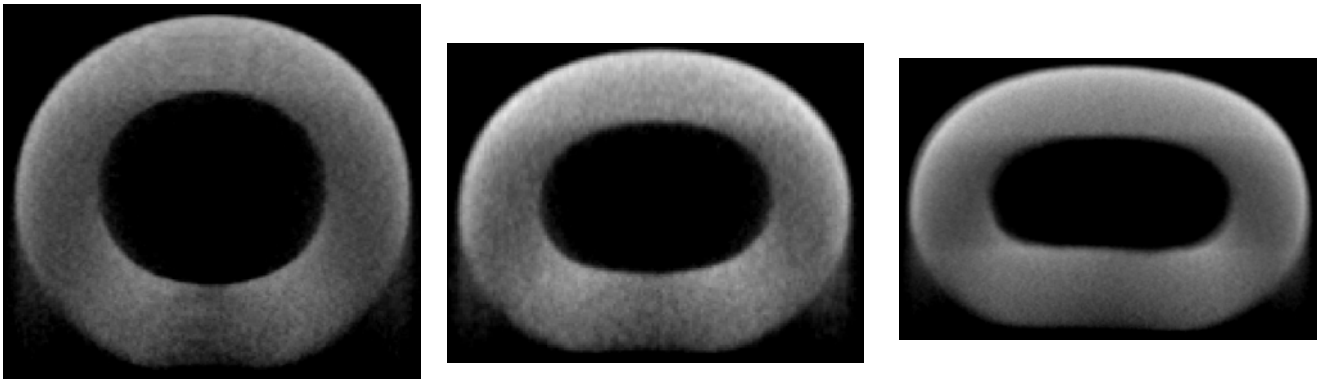

(a) 1 bend (b) 6 bends (c) 16 bends

Figure 4. X-ray computed tomography images of the pipe cross-sections

Table 2. Cross-sectional dimensions at horizontal centreline of Figure 1 for different deformation histories

Number of bend cycles	Major diameter (mm)		Minor diameter (mm)		Wall thickness (mm)			
	Outer	Inner	Outer	Inner	Outer	Inner	Side 1	Side 1
0	3.175	1.753	3.175	1.753	0.711	0.711	0.711	0.711
1	3.29	1.88	2.93	1.63	0.64	0.67	0.72	0.71
6	3.39	2.00	2.59	1.31	0.62	0.65	0.68	0.69
16	3.38	2.04	2.23	0.96	0.61	0.68	0.68	0.68

A further important issue relevant to residual stress assessment, not discussed in Ref [4], is the possibility of transverse residual stresses arising from the circumferential strains that result from deformation of the cross-section from a circular to the deformed shape during the cold forming process. The internal geometry of the pipes with 1, 6 and 16 bends, through the horizontal centreline, was revealed by X-ray CT images, which show that that the transverse residual strains could be of the order of -7.7% to 3.6%, -18% to 6.8% and -30% to 6.5% for the 1, 6 and 16 bend samples respectively. The range of values indicates the deformations, assuming and elliptical shape for the major and minor axes of the ellipse. The effect of this on the thermoelastic signal is currently being investigated as it is possible that exposure to negative plastic strain may have a different effect on the thermoelastic response than positive plastic strain. Indications of this being the case are present in the experimental data given in Ref. [5].

Thermoelastic damage analysis of pipe specimens

The work in the previous section indicates that in the quarter hard stainless steel pipes an assessment of damage based on changes in the thermoelastic constant is not possible. However, it may be possible to assess levels of material damage by examining the non-adiabatic behaviour of the test specimens [3]. In this section of work the potential of using this approach on these smaller scale pipes is explored. The CT has also shown that there are significant changes in the pipe geometry that will

cause changes in the stress field at the bend. Therefore it was decided to conduct TSA work that would compare the thermoelastic response from the specimens with a range of deformations exposed to the severe bending cycles, to assess if the level of deformation can be determined from the thermoelastic response. Although the existence of damage was not apparent in the CT data, in-service reports indicate that failures occur above 16 bend cycles. Therefore TSA data was collected at a range of frequencies range to assess if there were any significant departures in the response to indicate the presence of damage. In the TSA work specimens 1, 3, 5, 8, 12 and 16 were examined. The loading arrangement is shown in Figure 1.

The TSA tests on the deformed specimens were performed using an Instron servo-hydraulic test machine. A 1 kN load cell was fitted to the test machine as the loads required were very small to ensure the stresses remained elastic throughout the specimen [4]. As such low loads were required it was necessary to use position control to maintain a constant cyclic load during testing and hence minimise any variation in the thermoelastic response due to departures in the load cycle. A displacement range of 0.10 mm (equivalent to a load of approximately 23 N) was used to load the specimens at a variety of frequencies in the range 2.5 to 30 Hz, to assess if there was any dependence on loading frequency that indicates subsurface damage [3].

Even at these low load levels the motion of the test specimen was excessive when using the zoom lens, which precluded the use of data from the side view of the specimen, as shown in Figure 1. The data considered in this work was therefore the direct view of the outside of the bend, where the data is practically constant and blurring of the edges is not a problem. An example of the thermoelastic data considered in this section of work is given in Figures 5, 6 and 7, which show the in-phase (X), out-of-phase (Y) and phase data respectively for the most severely damaged specimen at loading frequencies of 2.5, 10 20 and 30 Hz.

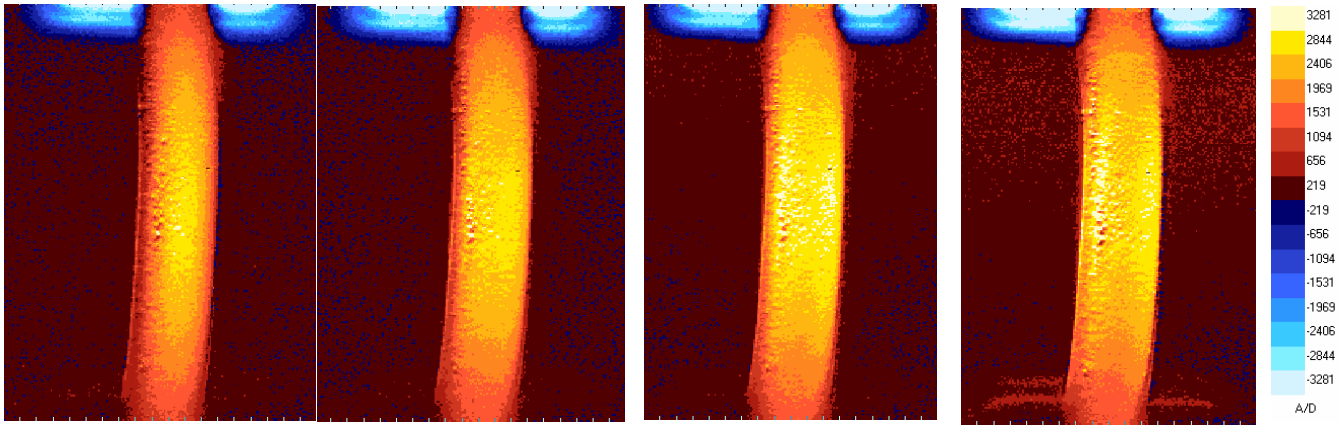

(a) 2.5 Hz (b) 10 Hz (c) 20 Hz (d) 30 Hz

Figure 5. In-phase images for the pipe subjected to 16 deformation cycles at a variety of loading frequencies

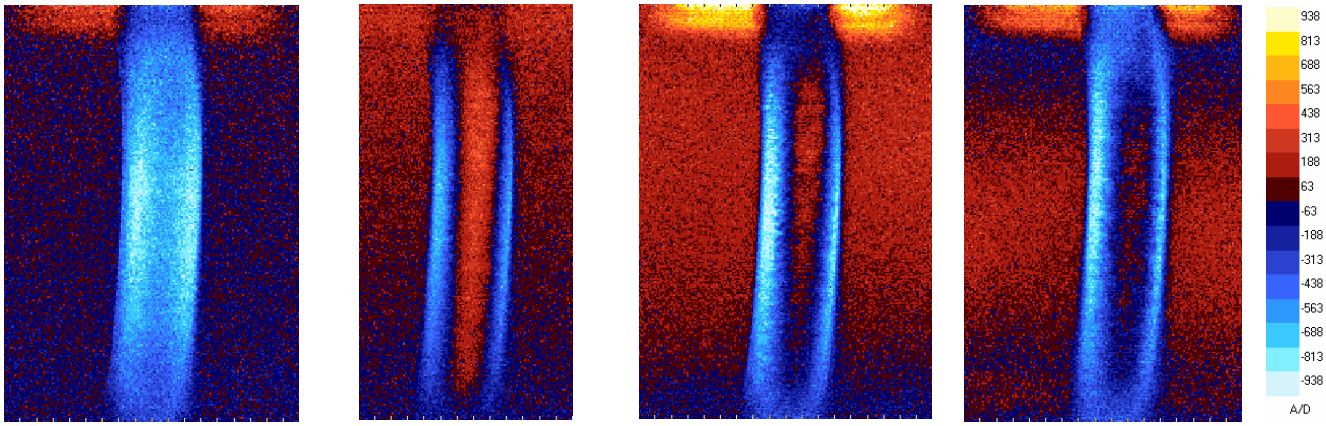

(a) 2.5 Hz (b) 10 Hz (c) 20 Hz (d) 30 Hz

Figure 6. Out-of-phase images for the pipe subjected to 16 deformation cycles at a variety of loading frequencies

Figure 5 shows that the in-phase (X) images for 10 to 30 Hz are similar in the central region of the pipe. The data selected for post-processing was a centrally located 10 by 10 pixel box. The variations in the X data for the specimens considered in this section of work is given in Figure 8. For the pipe subjected to 16 deformation cycles the X signal is essentially constant across the entire frequency range tested, from 2.5 to 30 Hz. The same insensitivity to loading frequency is apparent for the 12 bend specimen but for specimens with 8 bends and less there is a noticeable attenuation of the X signal at test frequencies less than 10 Hz, which increases with decreasing test frequency. This attenuation is greater for the specimens with smaller numbers of deformation cycles, see Figure 8. This suggests that non-adiabatic is occurring at frequencies less than 10 Hz for the least deformed specimens, i.e. those subjected to 1, 3 and 5 bends, however this is probably due to the through thickness stress gradient rather than damage.

The differences in the out-of-phase (Y) images for the most severely deformed pipe at different loading frequencies are much more pronounced and are significantly different at 2.5, 10, 20 and 30 Hz (see Figure 6). In general the Y signal peaks at a loading frequency of 10 Hz before reducing in a monotonic fashion with increasing loading frequency.

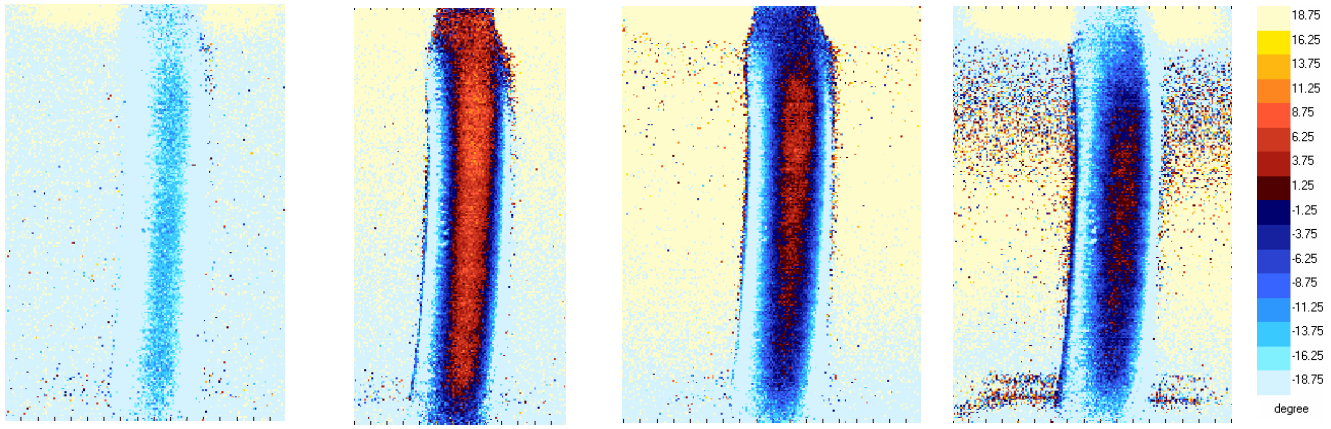

(a) 2.5 Hz (b) 10 Hz (c) 20 Hz (d) 30 Hz

Figure 7. Phase images for the pipe subjected to 16 deformation cycles at a variety of loading frequencies

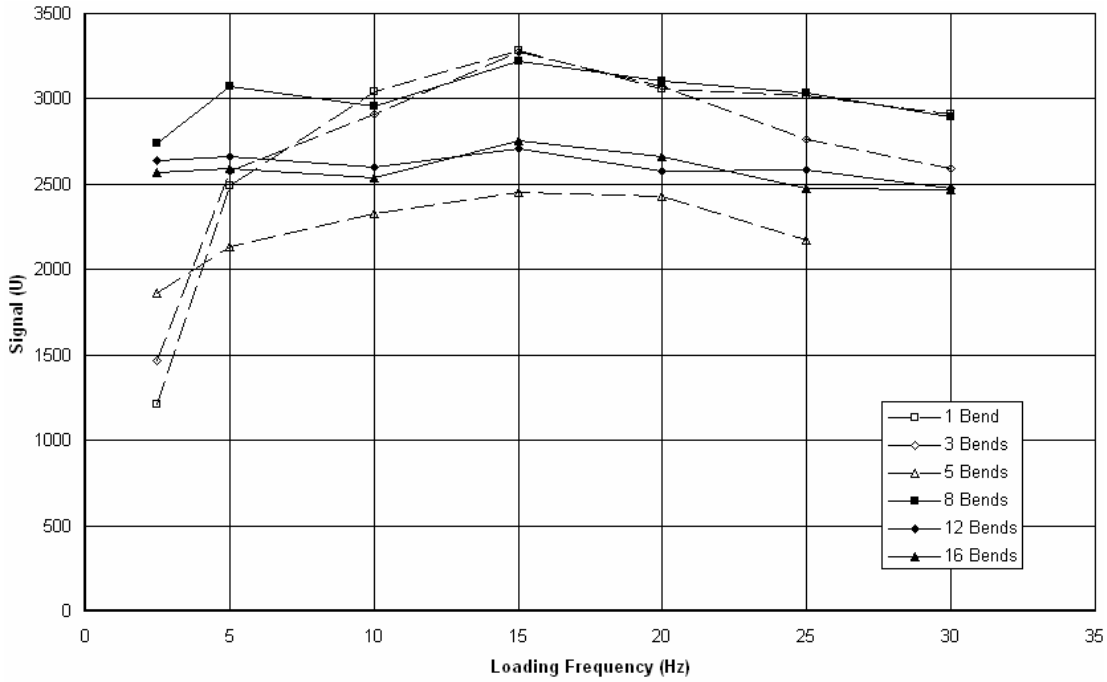

Figure 8. Comparison of in-phase signal from pipes with different deformation histories for different loading frequencies

Like the out-of-phase (Y) data the phase images throughout the frequency range considered are clearly different, see Figure 7. The trends in the phase data are similar to that for the Y data, and are shown in Figure 9. There is a monotonic decrease in phase angle from the peak that occurs at a loading frequency of 10 Hz with increasing loading frequency and a much more significant reduction at frequencies less than 10 Hz. There is a clear difference in the two groups of specimens tested on different days, which is not thought to be meaningful and could be corrected by a simple shift in the data. If this shift was applied the phase data would all fit within a ±10 degree band for loading frequencies between 5 and 30 Hz, with the significant reduction in phase at loading frequencies less than 5 Hz.

The TSA data has shown that there are no significant differences in the thermoelastic signal and hence stress from pipes with significant deformation histories. By approximating the deformed shape to an ellipse and considering the changes in the section modulus it is possible to estimate the changes in the applied bending stresses resulting from the geometry changes shown in the Figure 4. The bending stress for 6 and 16 bends were estimated to be 21% and 59% greater respectively when normalised against the calculation for 1 bend. This is not reflected in the TSA data and is the object of current work. Finally the TSA did not show ant significant non-adiabatic behaviour than may indicate the presence of damage.

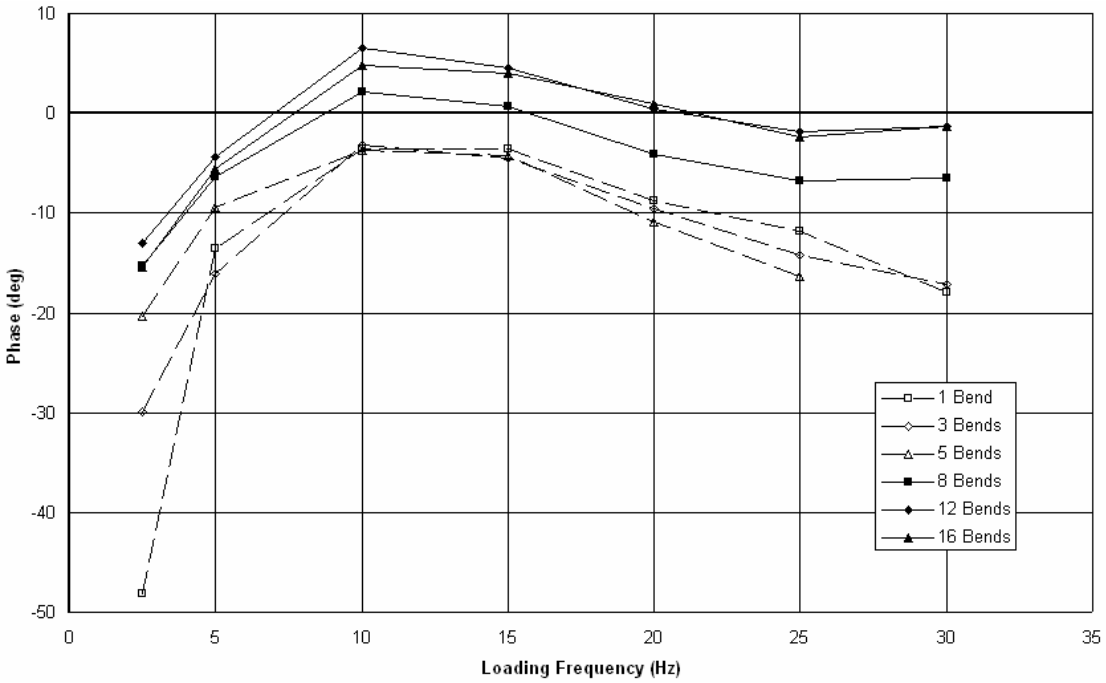

Figure 9. Comparison of phase data from pipes with different deformation histories for different loading frequencies

Closure

It has been shown that strain hardening is an important mechanism if the thermoelastic constant, K, of a metallic material is to change with plastic strain. The differences in K for strains of up to 20% were much more marked for an annealed stainless steel that strain hardens significantly in comparison to the as received cold drawn material that does not. X-ray computed tomography images have been used to measure the actual cross-sectional geometry of deformed pipes. This has shown that the cross-sectional geometry changes significantly as deformation cycles increase. The CT showed there is no damage greater than 10 μm in size at the internal surfaces of the pipe, even for a specimen that has been subjected to 16 deformation cycles. Thermoelastic stress analysis (TSA) has shown that there are no significant differences in the stress sum at the outside of the bend for pipes that have been subjected to 1, 3, 5, 8, 12 and 16 bends, although calculations based on the geometry of the specimen predict an increase in stress. The tests at different loading frequencies in the range 2.5 to 30 Hz has shown that the onset of non-adiabatic behaviour occurs for frequencies less than 10 Hz and becomes more pronounced as the frequency decreases.

Acknowledgements

The DeltaTherm 1410 system used in this work was loaded from the EPSRC equipment loan pool and this is gratefully acknowledged. The authors would also like to acknowledge Professor Ian Sinclair and Mr Andrew Moffat, who provided the X-ray computed tomography images in this work.

References

[1] Dulieu-Barton, J.M and Stanley, P., "Development and applications of thermoelastic stress analysis", Journal of Strain Analysis, **33**, 93-104 (1998).

[2] Stanley, P. and Chan, W. K., "Quantitative stress analysis by the means of the thermoelastic effect", Journal of Strain Analysis, **20**, 129-137 (1985).

[3] Sathon, N. and Dulieu-Barton, "Damage analysis of internal surface flaws using thermoelastic stress analysis", Key Engineering Materials, **293 – 294**, 279-286 (2005).

[4] Quinn, S., Tatum, P.J., Dulieu-Barton, J.M. and Eaton-Evans, J., Proceedings of SEM Annual Conference and Exposition on Experimental and Applied Mechanics, Saint Louis, Paper Reference 288 [10pp on CD] (2006).

[5] Quinn, S., Dulieu-Barton, J.M. and Langlands, J.M., "Progress in thermoelastic residual stress measurement", Strain, **40**, 127-133 (2004).